Available online at www.sciencedirect.com

ScienceDirect

Procedia Engineering 154 (2016) 609 – 616

Procedia Engineering

www.elsevier.com/locate/procedia

12th International Conference on Hydroinformatics, HIC 2016

Assessing impervious area ratios of grid-based land use classifications on the example of an urban watershed

Tatsuya Koga[a,*], Akira Kawamura[b], Hideo Amaguchi[b]

[a]*CTI Engineering Co; Ltd, 3-21-1, Nihonbashihamacho, Chuo-ku, Tokyo 103-8430, Japan*
[b]*Department of Civil and Environmental Engineering, Tokyo Metropolitan University, 1-1 Minami-Ohsawa, Hachioji, Tokyo 192-0397, Japan*

Abstract

When applying a distributed hydrological model in urban watersheds, grid-based land use classification data with 10 m resolution are typically used in Japan. Land use classifications into 17 categories are made without taking into account their impermeable properties. Thus, for such a grid-based urban hydrological model, the estimation of the Impervious Area Ratio (IAR) of each land use classification is a crucial factor for accurate runoff analysis in urban watersheds. However, so far IAR of each classification is estimated very roughly and applied in the corresponding hydrologic models almost empirically. Thus in order to assess the IAR accurately, we created a set of vector-based "urban landscape GIS delineation" data for a typical urban watershed in Tokyo using detailed land use recognition, which exactly delineated the pervious and impervious features into 20 land use types in the watershed. These vector data are used to improve the impervious area depiction of grid-based land use classifications. By superimposing the vector-based delineation map on the grid-based map, the IAR of each grid-based land use classification was estimated with very little uncertainty, after calculating the IARs of all grid cells in the entire urban watershed. As a result, we were able to calculate the frequency distribution of IAR for each land use classification as well as the spatial distribution of IARs for the urban watershed.

Peer-review under responsibility of the organizing committee of HIC 2016

Keywords: impervious area ratio; grid-based hydrologic model; land use classification; urban landscape GIS delineation; urban watershed; 10 m resolution

* Corresponding author. Tel.: +81-3-3668-0352; fax: +81-3-5695-1886.
E-mail address: t-koga@ctie.co.jp

Peer-review under responsibility of the organizing committee of HIC 2016
doi:10.1016/j.proeng.2016.07.559

1. Introduction

From a process description point of view, watershed hydrological models for different purposes can be classified into lumped and distributed models (Singh, 1995 [1]). Distributed models take explicit account of the spatial variability of processes, inputs, boundary conditions and watershed characteristics. In most distributed models, raster-based approaches for land-use characterization using Digital Elevation Model (DEM) have been developed (e.g. SHE (Abbott et al., 1986 [2]), GSSHA (Downer & Ogden, 2004 [3]), PCRaster (Karssenberg et al., 2010 [4])). The advantages of grid-based distributed models are their simple model structure and their use of watershed information that is generally readily available. Because of these advantages, grid-based distributed models are widely used. Especially in urban applications, direct runoff in each grid cell is usually calculated based on estimated fractions of impervious area or estimated runoff coefficients in different land use categories (e.g. Niehoff et al., 2002 [5]; Choi & Ball, 2002 [6]; Park et al., 2008 [7]). The Impervious Area Ratio (IAR) is the most important index representing the direct runoff characteristic of grid-based hydrological models. A proper estimation of the IAR of a grid cell (or of each land use category) is therefore crucial for accurate runoff simulation in urban systems, with their high degree of imperviousness (Leopold, 1968 [8]).

In Japan, grid-based hydrological models typically utilize readily available “digital map information data” published by the Geospatial Information Authority of Japan. In metropolitan regions, grid-based land use classification data on 10-m resolution are generally used for urban watershed hydrological models as the only source of basic data. However, as these data were established for the purpose of city planning, the impermeable properties of the grid cells are not taken into account. Each 10-m resolution grid cell is assigned only one dominant land use classification out of the 17 categories. Then, the IAR of the grid cell is set automatically according to its land use classification. Even in a small 10 m × 10 m grid cell, however, there may exist a wide range of pervious and impervious features, especially in urban watersheds in Japan (Amaguchi et al., 2012 [9]). This makes it more difficult to accurately estimate the IAR of each land use classification, let alone estimate the IARs of all the grid cells in the entire watershed. So far, no papers/reports have been published on accurately estimating IARs for the land use classifications and for all grid cells in the target urban watershed, because no reference GIS data exist for that purpose in Japan.

A number of studies have been published during the past few decades that try to identify the impervious surface areas in urban watersheds using remote sensing techniques such as satellite imagery and/or aerial photos. These studies proposed various methods (e.g. Slonecker et al., 2001 [12]; Thomas et al., 2003 [13]; Yang, et al., 2003 [14]; Yuan et al., 2008 [15]; Weng, 2012 [16]; Sugg et al., 2014 [17]). However, their methodologies need the highly accurate and precise calibration and validation surface data (i.e. the ground truthing data) of the watershed to be compared with in order to assess their estimation errors. The IAR estimates of a target urban watershed by remote sensing data generally involve not a small uncertainty (Civaco et al., 2006 [18]; Chabaeva et al., 2009 [19]).

Furthermore, indirect assessments of impervious surface via remote sensing data can be reasonably robust, but these generally require a ground truthing level-of-effort similar to manual methods (Yang 2002 [20]).

On the other hand, the recent advances in GIS technology, as well as data availability, open up new possibilities concerning urban runoff modelling. A few non-raster-based models have been developed from an urban morphology viewpoint that allow consideration of individual features in the urban environment. In contrast to current modelling approaches, which are generally based on grid data (e.g. Hsu et al., 2000 [21]; Ettrich et al., 2005 [22]; Dey and Kamioka, 2007 [23]; Cuo et al., 2008 [24]), we proposed and developed a new approach to simulate urban storm runoff and flood inundation with a vector-based watershed description that exactly delineated the pervious and impervious land surface features for a typical urban watershed in Tokyo, Japan (Amaguchi et al., 2012 [9]). This urban watershed-based methodology employs so-called “urban landscape GIS delineation” that faithfully describes the complicated urban land use features in detail (see Section 2.3).

In this study, we focused on the uncertainty of a model parameter IAR involved in grid-based distributed models. In order to assess the IARs of grid-based land use classifications in an urban watershed, we created a set of vector-based “urban landscape GIS delineation” data for a sub-watershed of the Kanda River, a densely-populated typical urban watershed in Tokyo, Japan. Taking full advantage of the vector-based data that exactly delineate the pervious and impervious features into 20 land use types in the watershed, we accurately estimated the IAR of each grid-based land use classification with 10-m resolution for the first time in Japan, after assessing the IARs of all grid cells in the

entire urban watershed. The frequency distribution of IAR for each land use classification and the spatial distribution of IARs among all the grid cells in the entire watershed were also clarified to improve our ability to assess IARs using the grid-based land use classification data.

2. LAND USE INFORMATION OF STUDY AREA

2.1. Study area

The study area selected for assessing the IARs of grid-based land use classifications is the upper Kanda watershed located in the Tokyo Metropolis, Japan. The Kanda River is the largest small to medium-sized river in Tokyo. It has a watershed area of 105.0 km^2, and a flow path extending to 25.5 km. The upper Kanda watershed area covers about 11.5 km^2, and the length of the river inside it is about 9 km long. The study area has been typically urbanized and densely populated, but these are still quite a few parks and forest-lands. The IAR of the study area has not yet been investigated.

2.2. Grid-based land use classifications

The grid-based land use classification data that are generally used as the basic data source for urban hydrological models are a set of land use data with 10 m × 10 m grid cells in the plane rectangular coordinate system. Table 1 presents the statistics of the study area represented by the grid-based land use classification. The table shows thus there are just 13 categories out of 17 are represented in the study area. Code numbers 2, 15, 16, 17 do not appear in this area. The study area consists of more than 113000 grid cells. Figure 1(a) shows the grid cell spatial distribution of the 13 land use classifications for the study area, in which the 100 m × 100 m grid area is enlarged. In Table 1 (columns 2-5), the “Low-rise residential land” is recognized as the most dominant, occupying about 51 % of the study area, followed by “Road” covering 12 % of the area. Urbanized areas occupy about 75 % of the watershed.

2.3. Vector-based land use types by urban landscape GIS delineation

The urban landscape GIS delineation divides land surface in the watershed into homogeneous features exactly as

Table 1. Statistics of the study area using the grid-based land use classification. TIA: total impervious area.

1	2	3	4	5	6	7
	Grid-based land use classifications				Urban landscape GIS delineation	
Classification *c*	Land use classification	*Number of grids Nc*	Area, A_c (m^2)	Area ratio, $\frac{A_c}{A}\times 100$ (%)	TIA (m^2)	IAR_c (%)
1	Forest	1 522	152 198	1.34	40 266	26.46
2	Paddy field	0	0	0.00	0	—
3	Dry field & other farmlands	2 477	247 698	2.18	74 470	30.06
4	Arranged land	27	2 700	0.02	1 700	62.97
5	Vacant land	4 731	473 094	4.17	317 040	67.01
6	Industrial land	695	69 499	0.61	60 189	86.60
7	Low-rise residential land	57 445	5 744 402	50.66	4 144 170	72.14
8	Densely developed low-rise residential land	2 908	290 795	2.56	227 504	78.24
9	Medium and high-rise residential land	2 635	263 496	2.32	170 042	64.53
10	Commercial land	7 068	706 790	6.23	569 609	80.59
11	Road	13 989	1 398 859	12.34	1 107 847	79.20
12	Park	9 673	967 288	8.53	273 978	28.32
13	Public facility	9 568	956 788	8.44	628 812	65.72
14	River, Lake, etc	656	65 599	0.58	61 137	93.20
15	Other land use	0	0	0.00	0	—
16	Sea	0	0	0.00	0	—
17	Non investigated area	0	0	0.00	0	—
	Total	N=113 394	A=11 339 205	100.00	7 676 763	IAR_e =67.70

seen on the surface map. The original data sources used in the urban landscape GIS delineation are the vector-based basic GIS delineation data and a 1/2500 topographic paper map provided by the Tokyo Metropolitan Government. The basic GIS delineation data only contain the polygon data of roads, rivers and buildings. Block polygons, which are defined as the areas enclosed by road and river polygons, were further divided into individual land use surface polygons manually according to their permeability using topographic maps, aerial photographs, and actual field survey data by the authors. As a result, the watershed was divided into a total of 20 land use type polygons, including road, river and building polygons, as shown in Table 2 (column 2). The impervious types are represented by the imperviousness index f_t = 1, whereas pervious types are represented by f_t = 0, as indicated in column 3 in Table 2.

Table 2 shows the statistics of the final land use types for the upper Kanda watershed using the urban landscape GIS delineation. The study area comprises more than 104000 homogeneous land surface features. This number is less than that of grid cells in Table 1. Figure 1(b) shows the spatial distribution of those land surface features into the

Table 2. Statistics of the study area using the grid-based land use classification.

1	2	3	4	5	6
Land use type, t	Land use type	Imperviousness index, f_t	Number of polygons	Area (m^2)	Area ratio (%)
1	Building	1.0	34 054	3 382 235	29.39
2	Parking lot (Pervious)	0.0	177	60 351	0.52
3	Parking lot (Impervious)	1.0	635	207 213	1.80
4	Athletic field (Pervious)	0.0	568	225 656	1.96
5	Athletic field (Impervious)	1.0	48	23 288	0.20
6	Forest	0.0	3 185	1 041 020	9.05
7	Grass	0.0	409	171 526	1.49
8	Field	0.0	483	188 587	1.64
9	Park	0.0	310	104 735	0.91
10	Cemetery	0.0	171	70 392	0.61
11	Paved area	1.0	1 157	379 521	3.30
12	Rail	1.0	570	149 388	1.30
13	Private premises (except buildings)	0.5	16 765	3 432 446	29.83
14	Tennis court (Pervious)	0.0	108	54 613	0.47
15	Tennis court (Impervious)	1.0	62	30 383	0.26
16	Bare land	0.0	117	52 714	0.46
17	Pool	1.0	27	11 750	0.10
18	Road	1.0	45 104	1 785 662	15.52
19	Pond	1.0	85	36 205	0.31
20	River	1.0	307	99 704	0.87
	Total	—	104 342	11 507 390	100.00

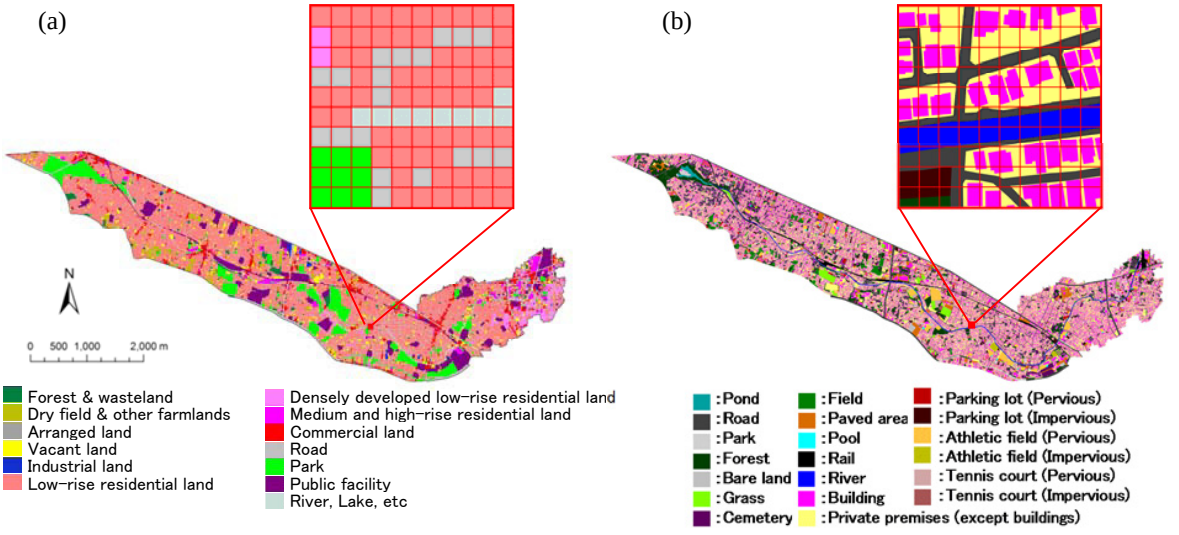

Fig. 1. Spatial distribution of (a) 13 grid-based land use classifications, and (b) individual land surface features of 20 land use types by urban landscape GIS delineation.

20 land use types, with the same 100 m × 100 m grid area as in Fig. 1(a) enlarged. From Table 2, the two largest land use types are “Private premises (except buildings)” and “Building”, with about 30 % of the area each, followed by “Road” (about 16 %) and “Forest” (about 9 %). These four types account for about 84 % of the watershed. From the enlarged part of the study area in Fig. 1(a) and (b), it is obvious that the grid-based land use classification is quite coarse compared to the urban landscape GIS delineation, for use in evaluating impermeable properties.

3. METHOD

Based on the urban landscape GIS delineation data, we calculate IAR in each grid cell. These values are then averaged over each of 13 grid-based land use classifications and then over the whole land use grid. In order to calculate the IAR (IAR_e) of the entire upper Kanda watershed as well as the IAR of the grid-based land use classification, first, the percentage IAR of each grid cell i (i = 1 to N ; N = 113394, the total number of grid cells in the watershed) (IAR_i,%) needs to be calculated. This is done by superimposing the vector-based delineation map on the grid-based map and IAR_i is calculated by Equation (1). The IAR_c (%) of the grid-based land use classification c (c = 1 to n_c; n_c = 17, the total number of grid-based land use categories) is estimated by Equation (3). The IAR_e (%) of the entire watershed is calculated by Equation (4).

$$IAR_i = \sum_{t=1}^{n_t} \frac{a_{it}}{a_i} f_t \times 100 \qquad (1) \qquad a_i = \sum_{t=1}^{n_t} a_{it} \qquad (2)$$

$$IAR_c = \frac{1}{N_c} \times \sum_{i=1}^{N_c} IAR_i \times 100 \qquad (3) \qquad IAR_e = \frac{1}{N} \sum_{i=1}^{N} IAR_i = \sum_{c=1}^{n_c} \frac{A_c}{A} IAR_c \qquad (4)$$

where n_t is the number of land use type t from the urban landscape GIS delineation (n_t = 20, shown in Table 2); f_t is the impervious index of the land use type t (shown in Table 2, column 3); a_{it} (m^2) is the area of land use type t in the grid cell i calculated by using the urban landscape GIS delineation data; a_i (m^2) is the area of the grid cell i (in this study, a_i = 100 m^2 for any i) by Equation(2); N_c is the total number of grid cells corresponding to land use category c; A_c (m^2) is the total area of grid-based land use category c (shown in Table 1, column 4); and A (m^2) is the total gridded area for the entire watershed.

4. RESULTS AND DISCUSSION

Figure 2(a) shows the frequency distribution of IAR_i for all grid cells (i = 1 to N; N = 113394) together with its

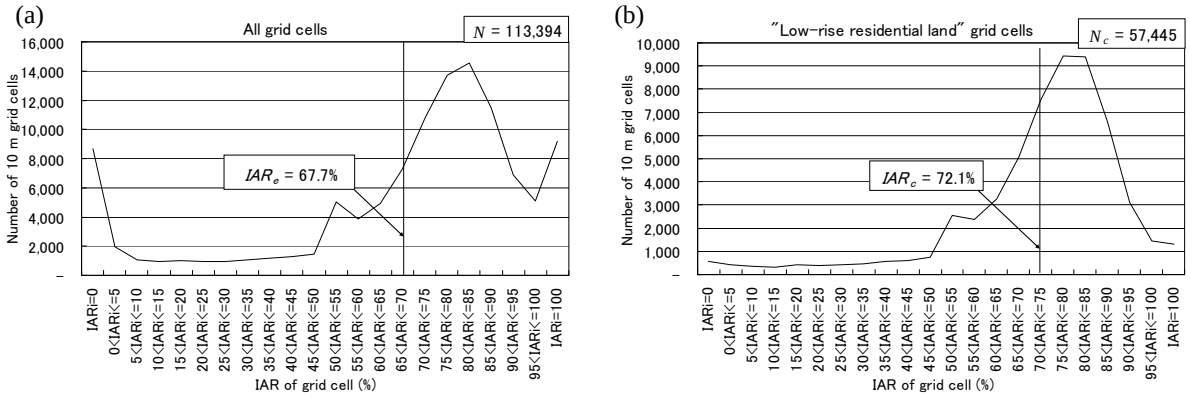

Fig. 2. Frequency distribution of IAR: (a) All grid cells, (b) "Low rise residential land" grid cells

Table 3. Area, area ratio and IAR of the 20 land use types by the urban landscape GIS delineation for the grid-based land use classifications of Fig. 2(a) and (b).

1	2	3	4	5	6	7	8	9
Land use type	Land use type	Impervious	Whole grid cells			"Low-rise residential" grid cells		
t		Index	Area	Area ratio	IAR	Area	Area ratio	IAR
		f_t	(m^2)	(%)	(%)	(m^2)	(%)	(%)
1	Building	1.0	3 364 050	29.67	29.67	2 190 177	38.13	38.13
2	Parking lot	0.0	60 322	0.53	0.00	19 954	0.35	0.00
3	Parking lot	1.0	206 529	1.82	1.82	55 036	0.96	0.96
4	Athletic field	0.0	225 656	1.99	0.00	4 032	0.07	0.00
5	Athletic field	1.0	23 288	0.21	0.21	503	0.01	0.01
6	Forest	0.0	1 034 359	9.12	0.00	402 335	7.00	0.00
7	Grass	0.0	171 506	1.51	0.00	27 550	0.48	0.00
8	Field	0.0	187 046	1.65	0.00	21 831	0.38	0.00
9	Park	0.0	103 925	0.92	0.00	12 985	0.23	0.00
10	Cemetery	0.0	70 392	0.62	0.00	1 671	0.03	0.00
11	Paved area	1.0	378 530	3.34	3.34	103 527	1.80	1.80
12	Rail	1.0	149 001	1.31	1.31	12 144	0.21	0.21
13	Private premises	0.5	3 403 818	30.02	15.01	2 200 893	38.31	19.16
14	Tennis court	0.0	54 612	0.48	0.00	497	0.01	0.00
15	Tennis court	1.0	30 383	0.27	0.27	3 428	0.06	0.06
16	Bare land	0.0	52 714	0.46	0.00	8 929	0.16	0.00
17	Pool	1.0	11 750	0.10	0.10	594	0.01	0.01
18	Road	1.0	1 675 437	14.78	14.78	667 854	11.63	11.63
19	Pond	1.0	36 205	0.32	0.32	0	0.00	0.00
20	River	1.0	99 681	0.88	0.88	10 461	0.18	0.18
Total		–	11,339,205	100.00	67.70	5 744 402	100.00	72.14

mean value (i.e. IAR_e). Additionally, Fig. 2(b) shows the distributions of IAR_i (i = 1 to N_c) for the grid cells with their mean values (i.e. IAR_c) corresponding to the land use classifications "Low-rise residential" as examples out of the 13 existing classifications represented in the watershed. Table 3 shows the area, area ratio and IAR for the 20 land use types using the urban landscape GIS delineation for the grid-based land use classifications of Fig. 2(a) and (b). From Fig. 2(a), the overall IAR of the entire watershed (IAR_e) is about 68 %, and the distribution has three major peaks. Besides the largest peak of IAR is in the range of 80-85%, but there are two unexpected peaks at 0 % and 100 %. This was clarified from the investigation that about 9000 completely impervious grid cells mainly came from the land use classifications "Public facilities" and "Road", which were completely covered by impervious "Building" and "Road" land use types, respectively. However, there were about 9000 completely pervious grid cells. These were mainly grid cells in the "park", "Dry field & other farmland" and "Forest" classifications. In Fig. 2(b), for the "Low-rise residential land" grid cells, there is just one major peak in the same range as in Fig. 2(a), but, in contrast, there are only few grid cells with 0% or 100% IAR values.

Table 1 (columns 6 and 7) shows the calculation results of TIA, IAR_c for each grid-based land use classification and the results for the entire watershed (IAR_e). In order to investigate the imperviousness characteristics of each grid-based land use classification, we examined the most dominant classification: "Low-rise residential land". From Table 3 (columns 7-9), almost all 19 land use types defined by the urban landscape GIS delineation are mixed in the "Low-rise residential land" grid cells. In addition, actual buildings occupy only about 38 % of the "Low-rise residential land" area, and there are many pervious areas such as "Private premises (except buildings)" and "Forest" in this classification.

The spatial IAR distribution for all the cells calculated using the urban landscape GIS delineation, in which each individual cell has its own value, is shown in Fig. 3(a) as 20-colour gradation. Figure 3(b) shows the spatial distribution of IAR_c of grid cells, given as the mean values of their corresponding grid-based land use classifications (Table 1, column 7); thus the figure contains just 13 colours. Figure 3(a) shows a wide range of IAR values, from 0 % to 100 % distributed in the watershed, with both impervious (close to 100 % IAR) and pervious (close to 0 % IAR) grid cells being naturally dominant. When applying grid-based distributed models, setting the true IAR value for each grid cell as shown in Fig. 3(a), is the most suitable, but it is almost impossible in actual practice unless the urban landscape GIS delineation data are available. Therefore, IAR values are generally defined based on the grid-based land use classifications, in which one land use classification is assigned one IAR value. Figure 3(b) shows the distribution of those IAR values (IAR_c), as given in Table 1 (column 7) for the classifications, from which the lowest

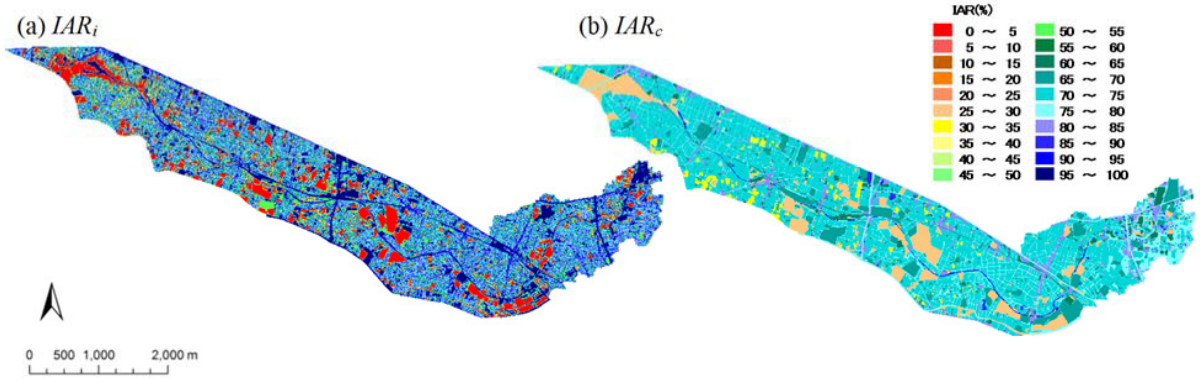

Fig. 3. Spatial distribution of (a) IAR of each grid cell (IARi) calculated using the urban landscape GIS delineation, (b) IARs of grid cells (IARc) assigned as the mean values of their corresponding grid-based land use classifications.

IAR value is about 26 % for “Forest”, and the highest is about 93 % for “River, Lake, etc.”. These estimated values (Table 1, column 7) will be used in practice as reference IAR values for a grid-based urban distributed hydrological model. Figure 3(b) is actually the best set of IARs from a practical point of view, even though the spatial distribution of IARs mainly ranges from about 60 % to 80 %, eliminating 0 % and 100 % values.

5. CONCLUSION

We estimated the Impervious Area Ratios (IARs) of grid-based land use classifications at 10 m × 10 m resolution in an urban watershed with very high accuracy using vector-based precisely homogeneous land surface feature data implemented by the urban landscape GIS delineation technique. The IAR is a critical factor in calculating direct runoff using grid-based distributed hydrological models. The results were used to assess the error inherited in distinguishing pervious and impervious area estimates from classical grid-based land use classification. We also analysed the impermeable characteristics of grid-based land use classifications in the upper Kanda watershed, a densely populated typical urban watershed, and found that a wide variety of land surface features with different impermeable properties were mixed within all land use classifications. The analysis showed the frequency distributions of IARs for all grid cells and for the grid cells of each land use classification. As a result, the overall IAR of the entire upper Kanda watershed was accurately estimated to be about 68 %, which was unknown until now. The actual spatial distribution of IARs in the watershed was also presented, together with a practical spatial distribution created by setting the IARs of each land use classification as their constant mean values. The distributions were quantitatively assessed. It is suggested that IAR should be accurately estimated for each urban watershed by creating a set of vector-based urban landscape GIS delineation data.

It is reasonable to say that the IARs obtained in this study are applicable for other highly populated urban watersheds if the impermeable properties are similar to the study area in this paper. The methodology presented here for calculating IARs would greatly contribute to improving simulation accuracy by a grid-based distributed hydrological model. In addition, the developed urban landscape GIS delineation data may be effectively used as ground truthing data to evaluate identified impervious areas obtained by remote sensing techniques. The main disadvantage of this methodology, however, is time and effort required to create the vector-based urban landscape GIS delineation data, in which individual land use surface polygons have to be manually delineated according to their permeability. At present, the authors already attempted to develop an automated delineation algorithm (Tanouchi et al., 2014 [26]). The ground truthing data created by such an automated algorithm would greatly contribute to accurate evaluation of IARs used in grid-based hydrological models.

Acknowledgements

This study was carried out as part of the research project "Solutions for water-related problems in Asian Metropolitan areas" supported by the Tokyo Metropolitan Government, Japan (represented by Dr. Akira Kawamura). We are very grateful to the reviewers for their dedicated corrections and suggestions, which have greatly contributed to marked improvements in the content of our research project.

References

[1] Singh VP. Watershed modeling. In: Singh VP, editors. *Computer Models of Watershed Hydrology*, Colorado: Water Resources Publications; 1995, Chapter 1.
[2] Abbott MB, Bathurst JC, Cunge JA, O'Connel PE, Rasmussen J. An introduction to the European hydrological system – Systeme hydrologique Europeen, "SHE", 1: history and philosophy of a physically-based, distributedmodelling system. *Journal of Hydrology* 1986; 87: 45-59.
[3] Downer CW, Ogden FL. GSSHA: model to simulate diverse stream flow producing processes. *Journal of Hydrologic Engineering* 2004; 9(3): 161-174.
[4] Karssenberg D, Schmitz O, Salamon P, De Jong K, Bierkens MFP. A software framework for construction of process-based stochastic spatio-temporal models and data assimilation. *Environmental Modelling & Software* 2010; 25: 489-502.
[5] Niehoff D, Fritsch U, Bronstert A. Land-use impacts on storm-runoff generation: scenarios of land-use change and simulation of hydrological response in meso-scale catchment in SW-Germany. *Journal of Hydrology* 2002; 267: 80–93.
[6] Choi KS, Ball EB. Parameter estimation for urban runoff modeling. *Urban Water* 2002; 4(1): 31-41.
[7] Park SY, Lee KW, Park IH, Ha SR. Effect of the aggregation level of surface runoff fields and sewer network for a SWMM simulation. *Desalination* 2008; 226: 328-337.
[8] Leopold LB. Hydrology for Urban land Planning. *US Geological Survey Circular* 1968; 554: 1-18.
[9] Amaguchi H, Kawamura A, Jonas O, Takasaki T. Development and testing of a distributed urban storm runoff event model with a vector-based catchment delineation. *Journal of Hydrology* 2012; 420-421: 205-215.
[10] Public Works Research Institute. Development of physically-based model for water and heat cycles in urban watershed. *Technical Note of PWRI* 2000; 3713: 51 (in Japanese).
[11] Public Works Research Institute. Handbook of WEP model (trial edition) 2002; 31 (in Japanese).
[12] Slonecker ET, Jennings DB, Garofalo D. Remote sensing of impervious surfaces: A review. *Remote Sensing Reviews* 2001; 20(3): 227-255.
[13] Thomas N, Hendrix C, Congalton RC. A comparison of urban mapping methods using high-resolution digital imagery. *Photogrammetric Engineering & Remote Sensing* 2003; 69(9): 963-972.
[14] Yang L, Xian G, Klaver JM, Deal B. Urban land-cover change detection through sub-pixel imperviousness mapping using remotely sensed data. *Photogrammetric Engineering & Remote Sensing* 2003; 69(9): 1003-1010.
[15] Yuan F, Wu S, Bauer ME, Comparison of spectral analysis techniques for impervious surface estimation using Landsat imagery. *Photogrammetric Engineering & Remote Sensing* 2008; 74(8): 1045-1055.
[16] Weng Q. Remote sensing of impervious surfaces in the urban areas: requirements, methods, and trends, *Remote Sensing of Environment* 2012; 117: 34-49.
[17] Sugg ZP, Finke P, Goodrich DC, Moran MS, Yool SR. Mapping impervious surfaces using object-oriented classification in a semiarid urban region. *Photogrammetric Engineering & Remote Sensing* 2014; 80(4): 343-352.
[18] Civco D, Chabaeva A, Hurd J. A comparison of approaches to impervious surface characterization. *Proc. IEEE Int'l Geoscience and Remote Sensing Symp* 2006; 4.
[19] Chabaeva A, Civco D, Hurd J. Assessment of impervious surface estimation techniques. *Journal of Hydrolic Engineering* 2009; 14(4): 377-387.
[20] Yang X. Satellite monitoring of urban spatial growth in the Atlanta metropolitan area. *Photogrammetric Engineering & Remote Sensing* 2002; 68(7): 725-734.
[21] Hsu MH, Chen SH, Chang TJ. Inundation simulation for urban drainage basin with storm sewer system. *Journal of Hydrology* 2000; 234(1-2): 21-37.
[22] Ettrich N, Steiner K, Thomas M, Pothe R, Surface models for coupled modelling of runoff and sewer flow in urban areas. *Water Science & Technology* 2005; 52: 25-33.
[23] Dey AK, Kamioka S. An integrated modeling approach to predict flooding on urban basin. *Water Science & Technology* 2007; 55(4): 19-29.
[24] Cuo L, Lettenmaier1 DP, Mattheussen BV, Storck P, Wiley M. Hydrologic prediction for urban watersheds with the distributed hydrology-soil-vegetation model. *Hydrological Processes* 2008; 22(21): 4205-4213.
[25] Melching CS. Reliability estimation. In: Singh VP, editors. *Computer Models of Watershed Hydrology*, Colorado: Water Resources Publications; 1995, 69-118.
[26] Tanouchi H, Amaguchi H, Kawamura A, Nakagawa N, Koga T. Study on an automated construction method of minute road segments aiming at urban storm runoff analysis, *Theory and Applications of GIS* 2014; 22(2): 25-34.